

CFD Simulations of a Regenerative Process for Carbon Dioxide Capture in Advanced Gasification Based Power Plants

Shahin Zarghami, Hamid Arastoopour, Javad Abbasian, Emadoddin Abbasi, Emad Ghadirian

Illinois Institute of Technology, Chicago, IL

Current Program Objective

The overall objective of the program is to develop a Computational Fluid Dynamic (**CFD**) model and to perform CFD simulations to describe the heterogeneous gas-solid absorption and regeneration and WGS reactions in the context of multiphase CFD for a regenerative magnesium oxide-based (**MgO-based**) process for simultaneous removal of CO_2 and enhancement of H_2 production in coal gasification processes.

Scope of Work

The Project consists of the following four (4) tasks:

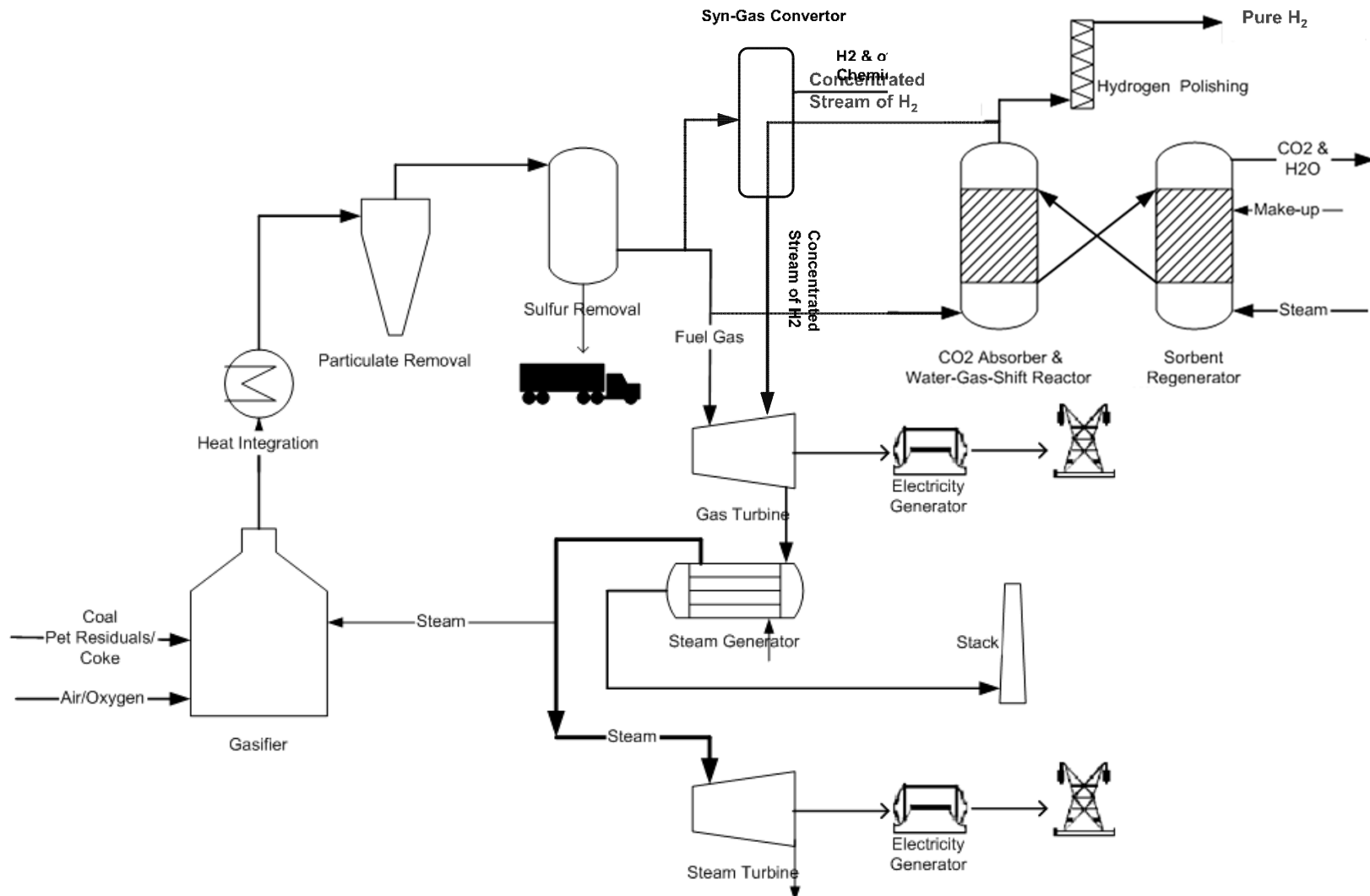
Task1. Development of a CFD/PBE model accounting for the particle (sorbent) porosity distribution and of a numerical technique to solve the CFD/PBE model. (Completed)

Task2. Determination of the key parameters of the absorption and regeneration and WGS reactions. (Close to Completion)

Task3. CFD simulations of the regenerative carbon dioxide removal process. (Close to Completion)

Task4. Development of preliminary base case design for scale up. (In Progress)

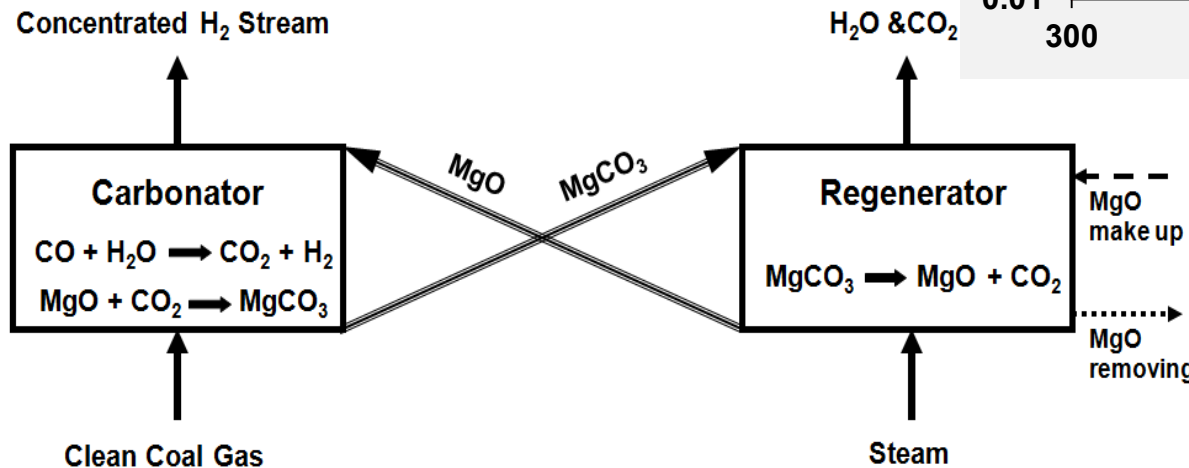
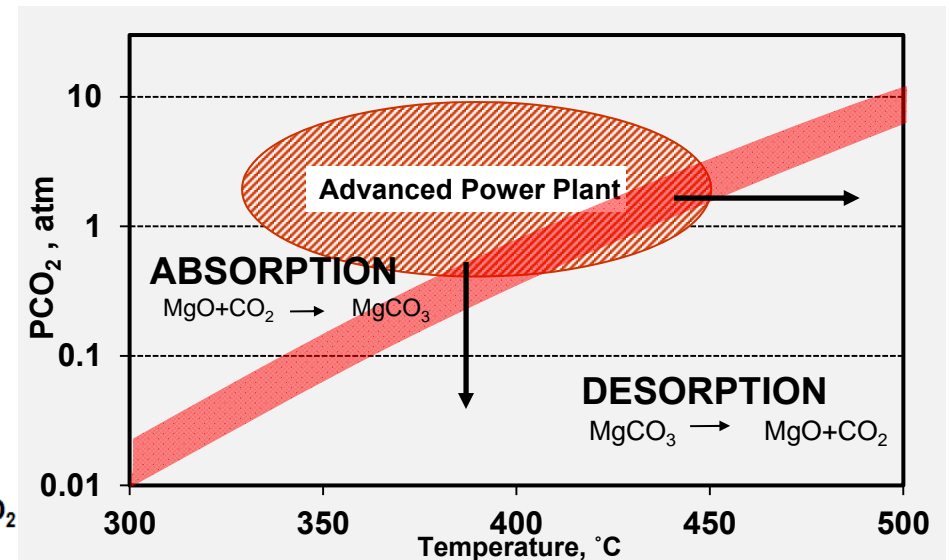
Schematic Diagram of a Typical IGCC Process



Regenerable Sorbent Approach

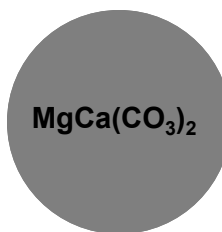
Process Economics is highly dependent on the CO₂ Sorbent properties

- CO₂ absorption Temperature (300 - 450 °C)
- Simple regeneration
- Sulfur and Steam Resistant
- Sorbent Cost (per cycle)



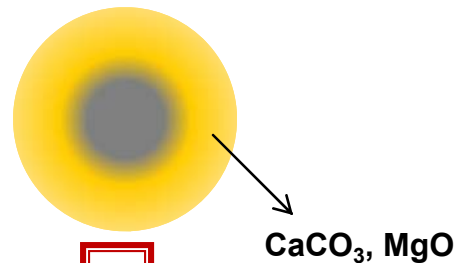
Sorbent Preparation Procedure

Dolomite



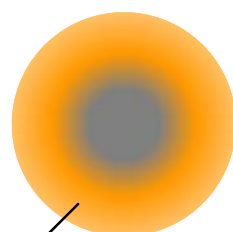
Fresh Dolomite

Half- Calcined Sorbent



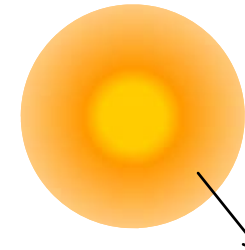
Modified Dolomite

Impregnated Sorbent



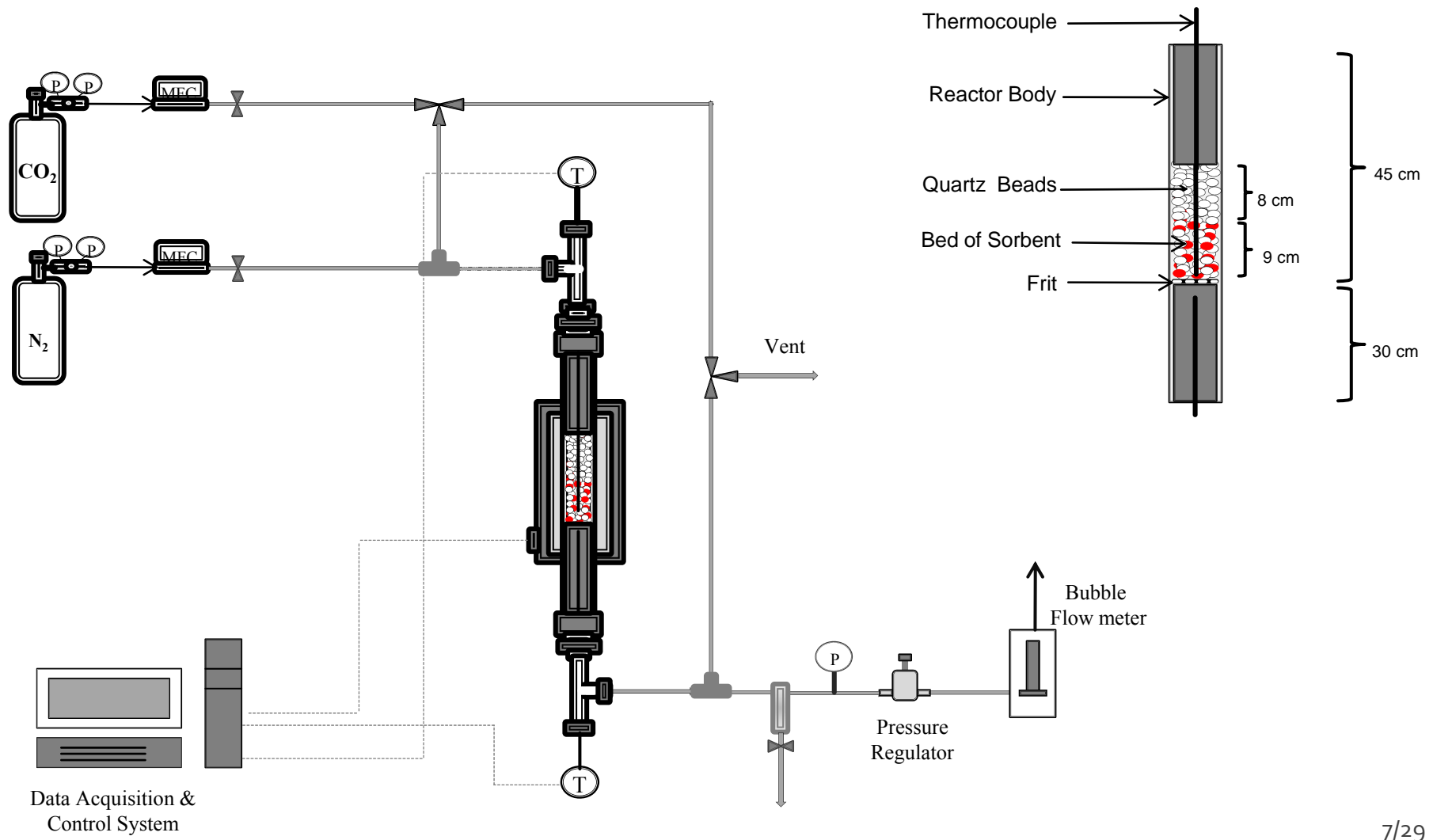
$\text{CaCO}_3, \text{MgO},$
 $\text{Mg(OH)}_2, \text{K}_2\text{CO}_3$

Re-Calcination

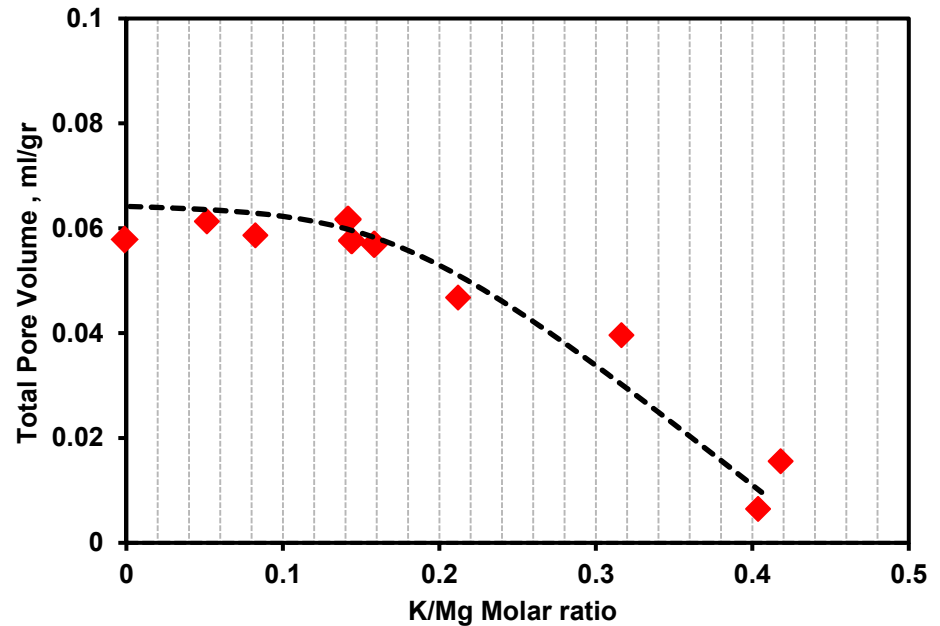
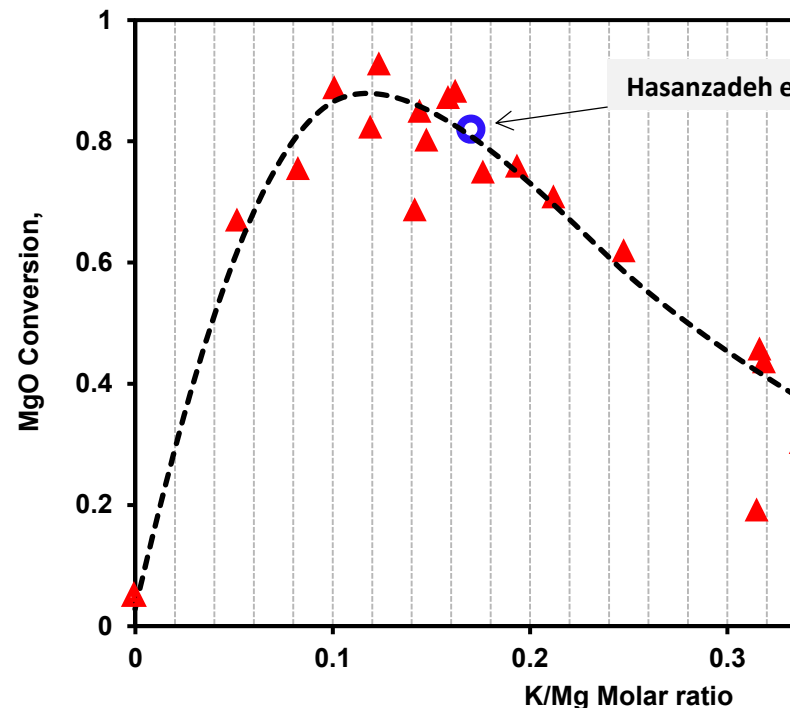


$\text{CaCO}_3, \text{MgO}, \text{K}_2\text{CO}_3$

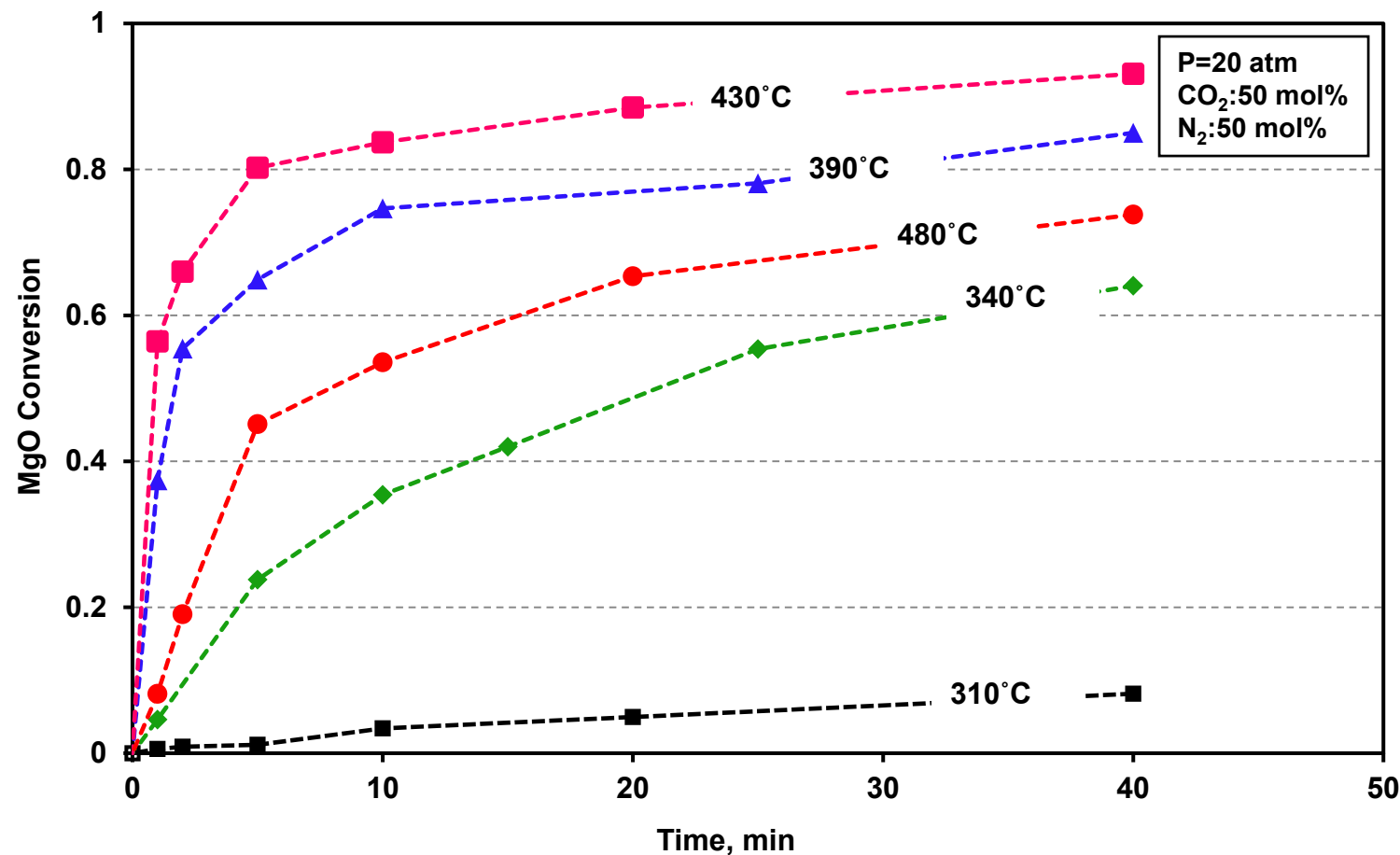
Experimental Setup: Dispersed Bed Reactor



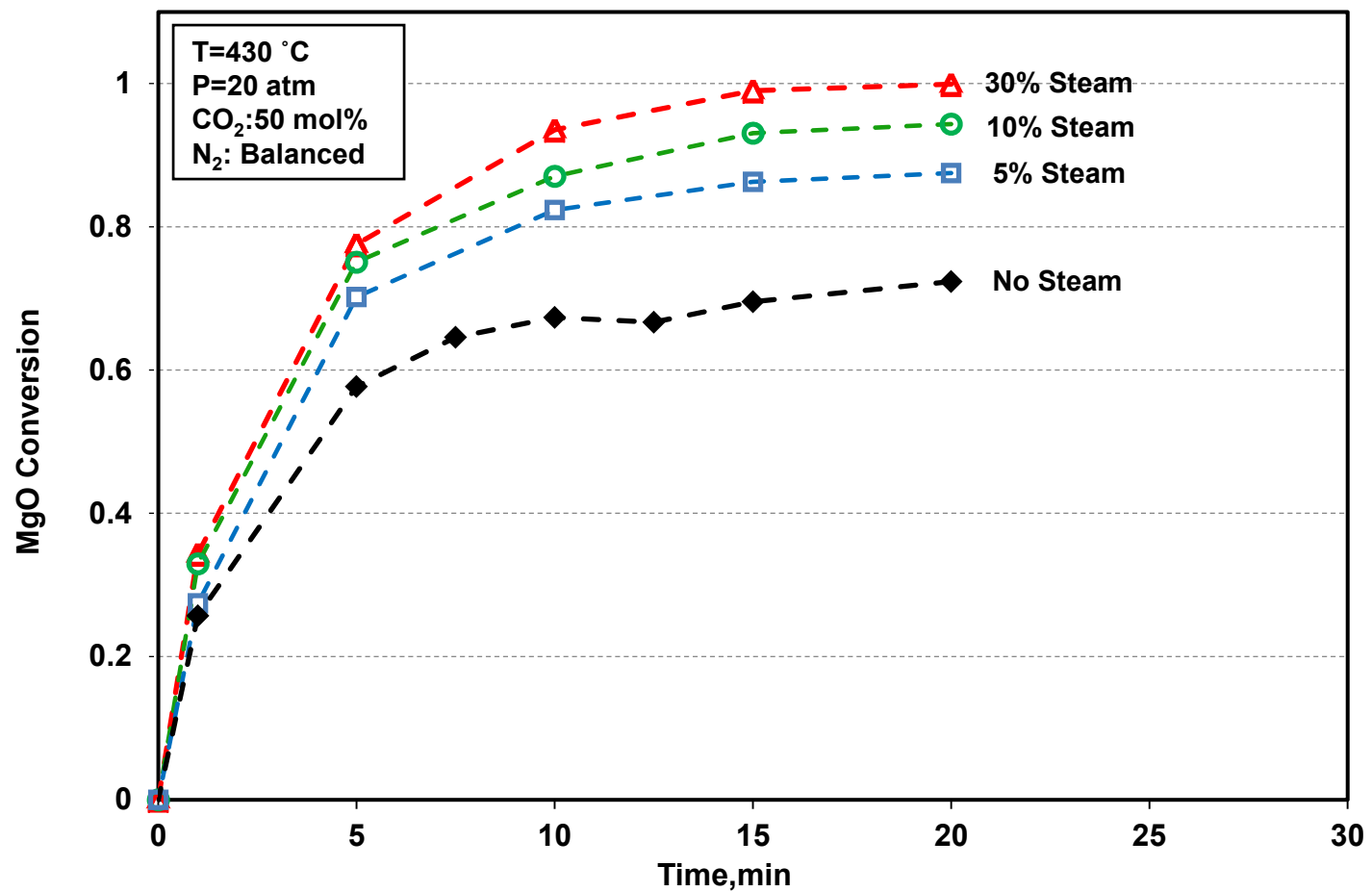
Effect of Potassium Concentration on Sorbent Reactivity and Capacity



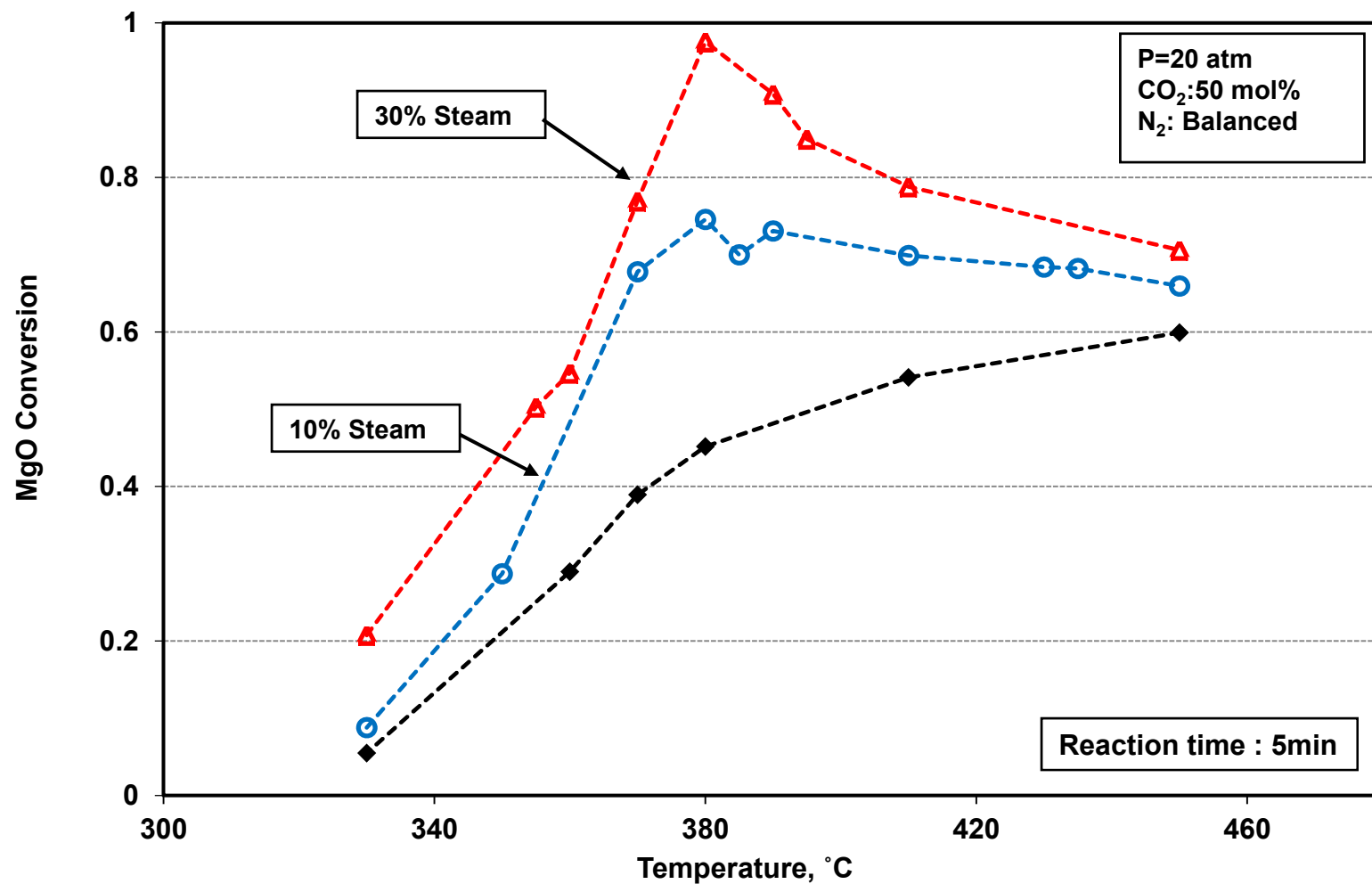
Effect of Temperature on Sorption



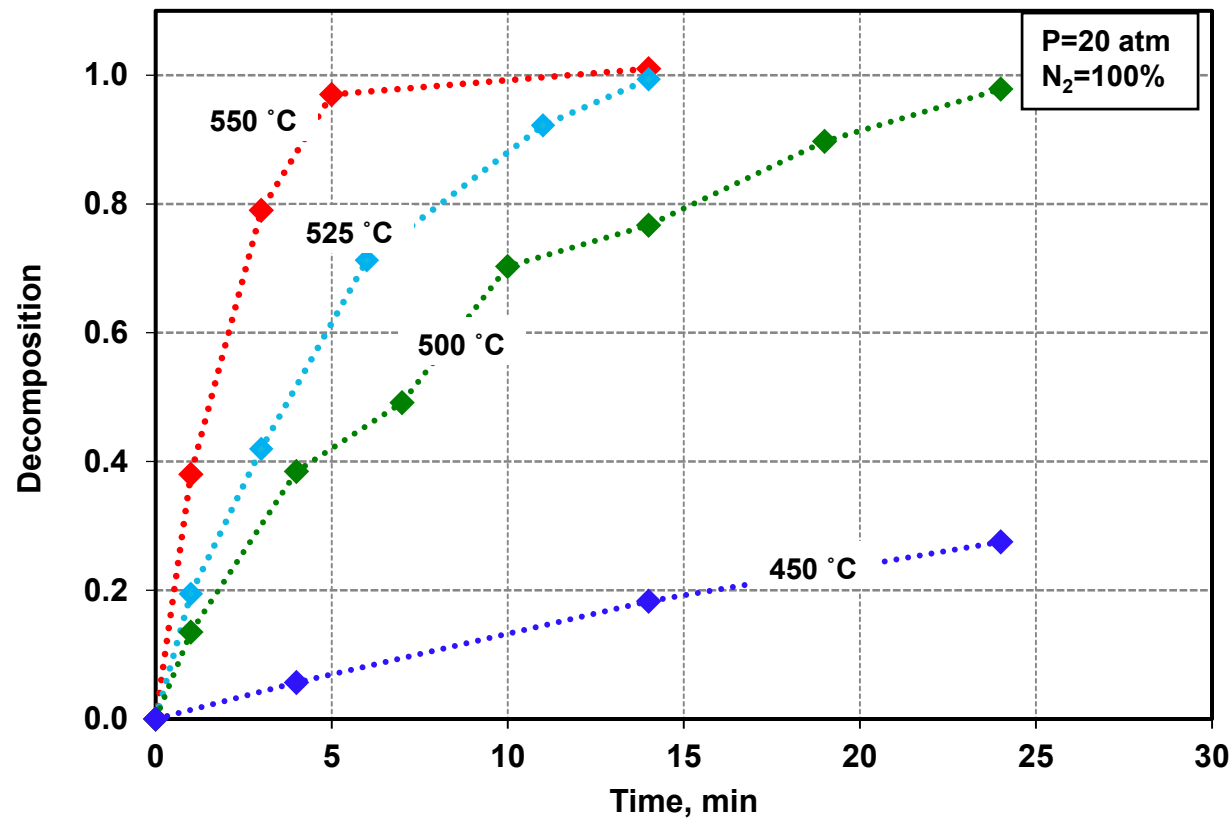
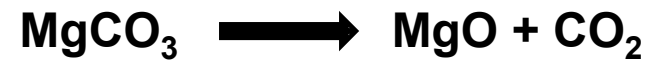
Effect of Steam on Reactivity



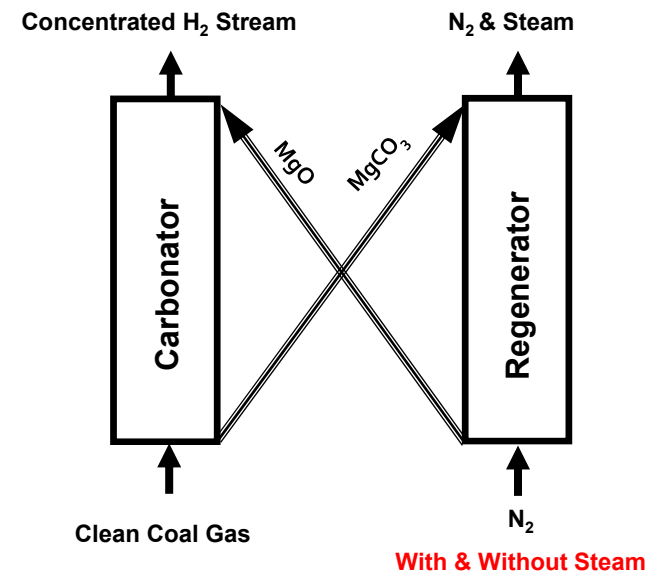
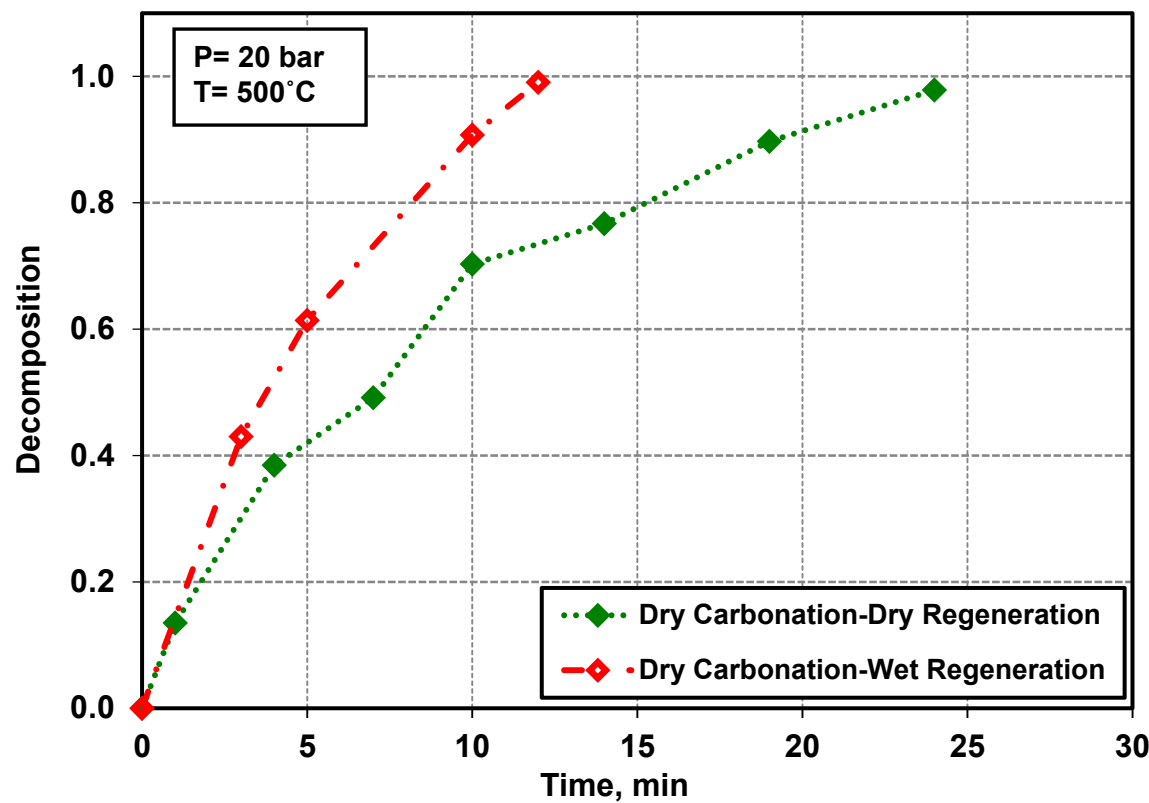
Effect of Steam on Reactivity



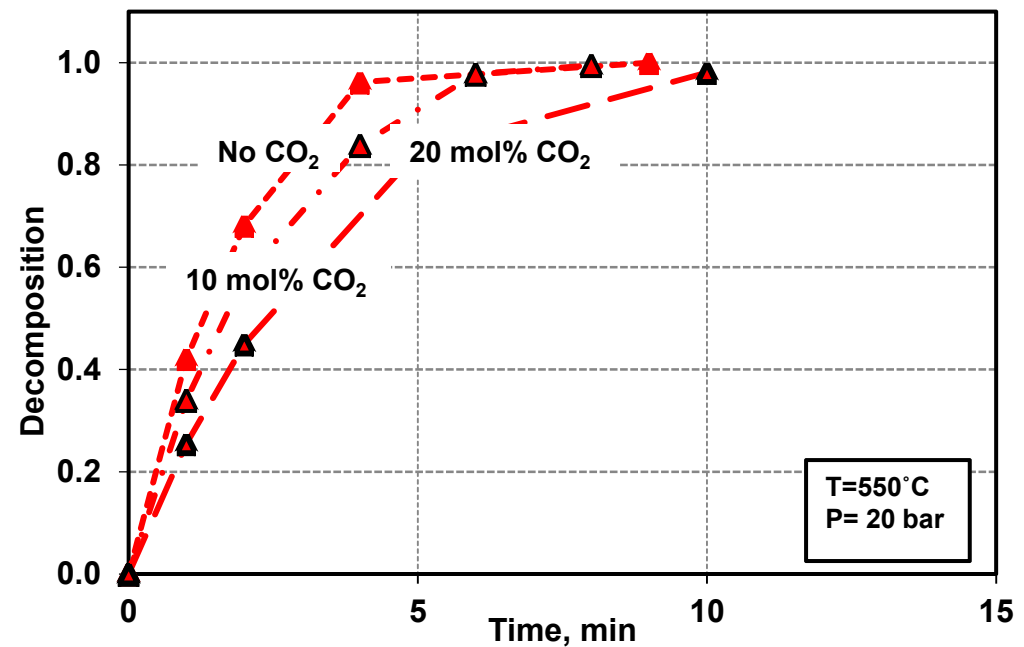
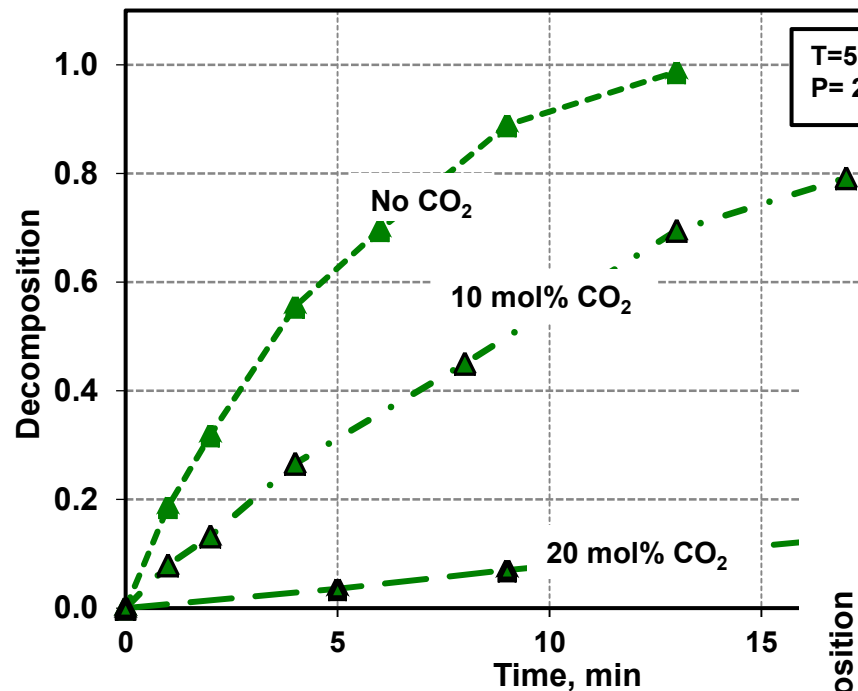
Effect of Temperature on Sorbent Decomposition



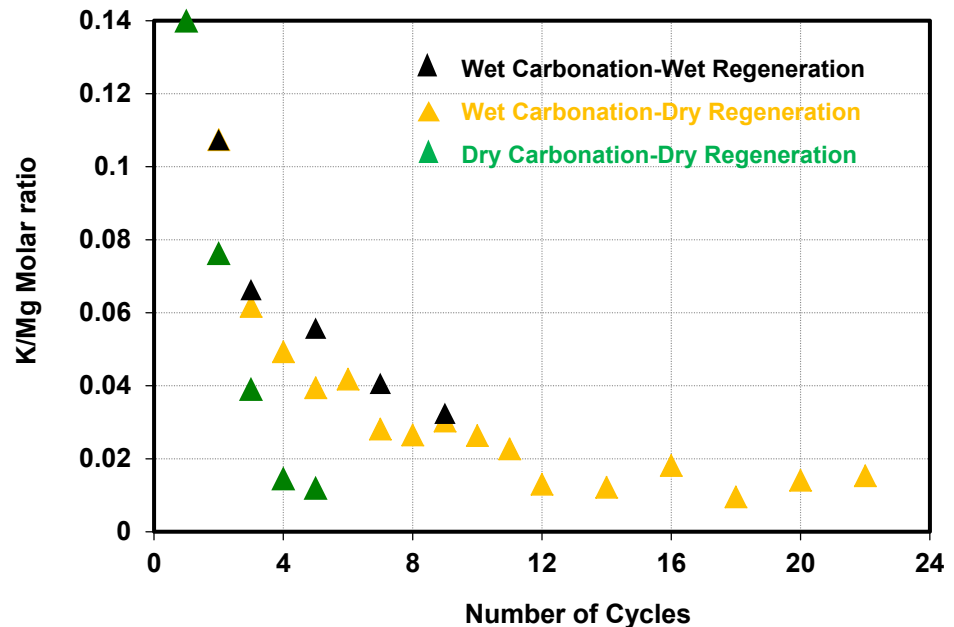
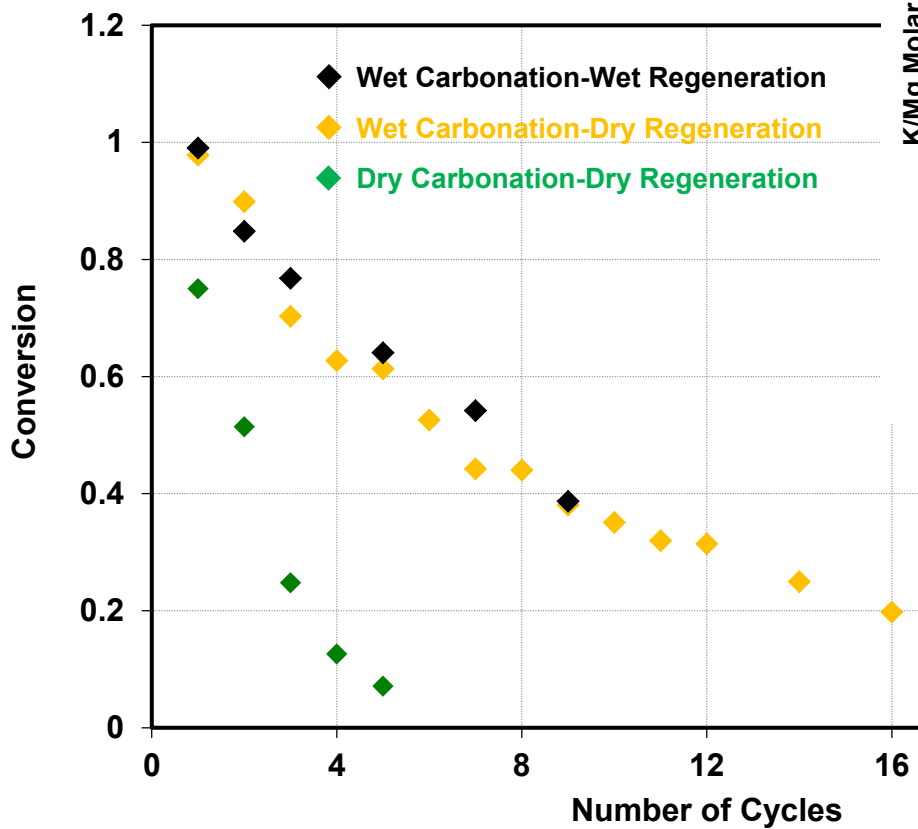
Effect of Steam on the Rate of Decomposition



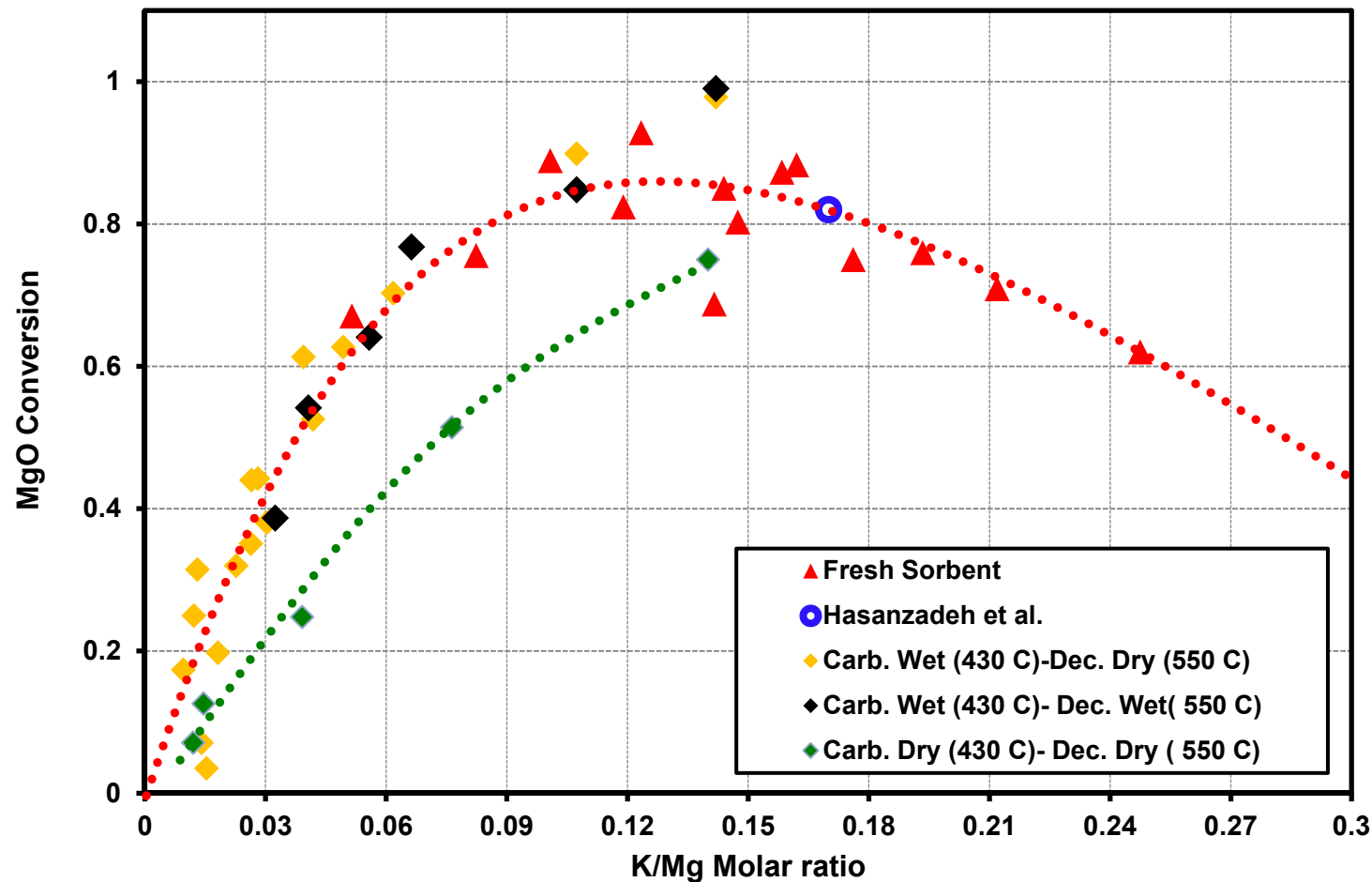
Effect of CO₂ on sorbent Regenerability



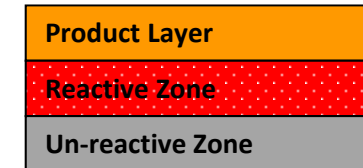
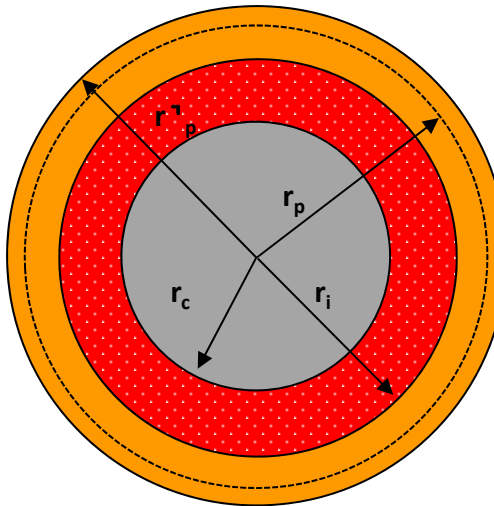
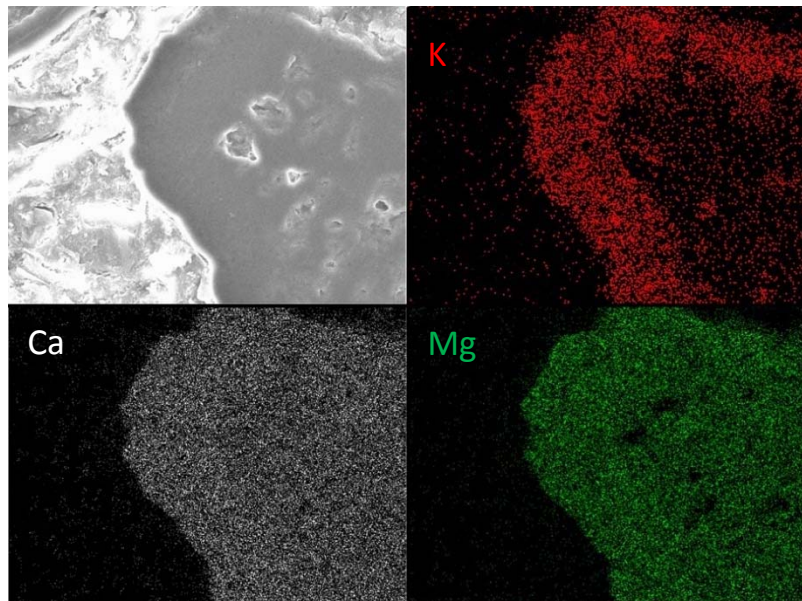
Effect of Steam on Sorbent Regenerability and Durability



Effect of Potassium Concentration on Sorbent Capacity



Variable Diffusivity Shrinking Core Model with Expanding product layer



$$Z = \frac{\rho_{product} \cdot M_{react}}{\rho_{react} \cdot M_{product}} \quad r_p = r_p' \sqrt[3]{(1-X) + ZX}$$

$$D_e \left[\frac{1}{r^2} \frac{\partial}{\partial r} \left(r^2 \frac{\partial C}{\partial r} \right) \right] = 0$$

$$B.C.1: \quad C = C_b \quad @ r = r_p^*$$

$$B.C.2: \quad D_e \frac{\partial C}{\partial r} = k_s (C_i - C_e) \quad @ r = r_i$$

$$r_{MgO} = -\frac{1}{4\pi r_i^2} \frac{dN_{MgO}}{dt} = k_s (C_i - C_e)$$

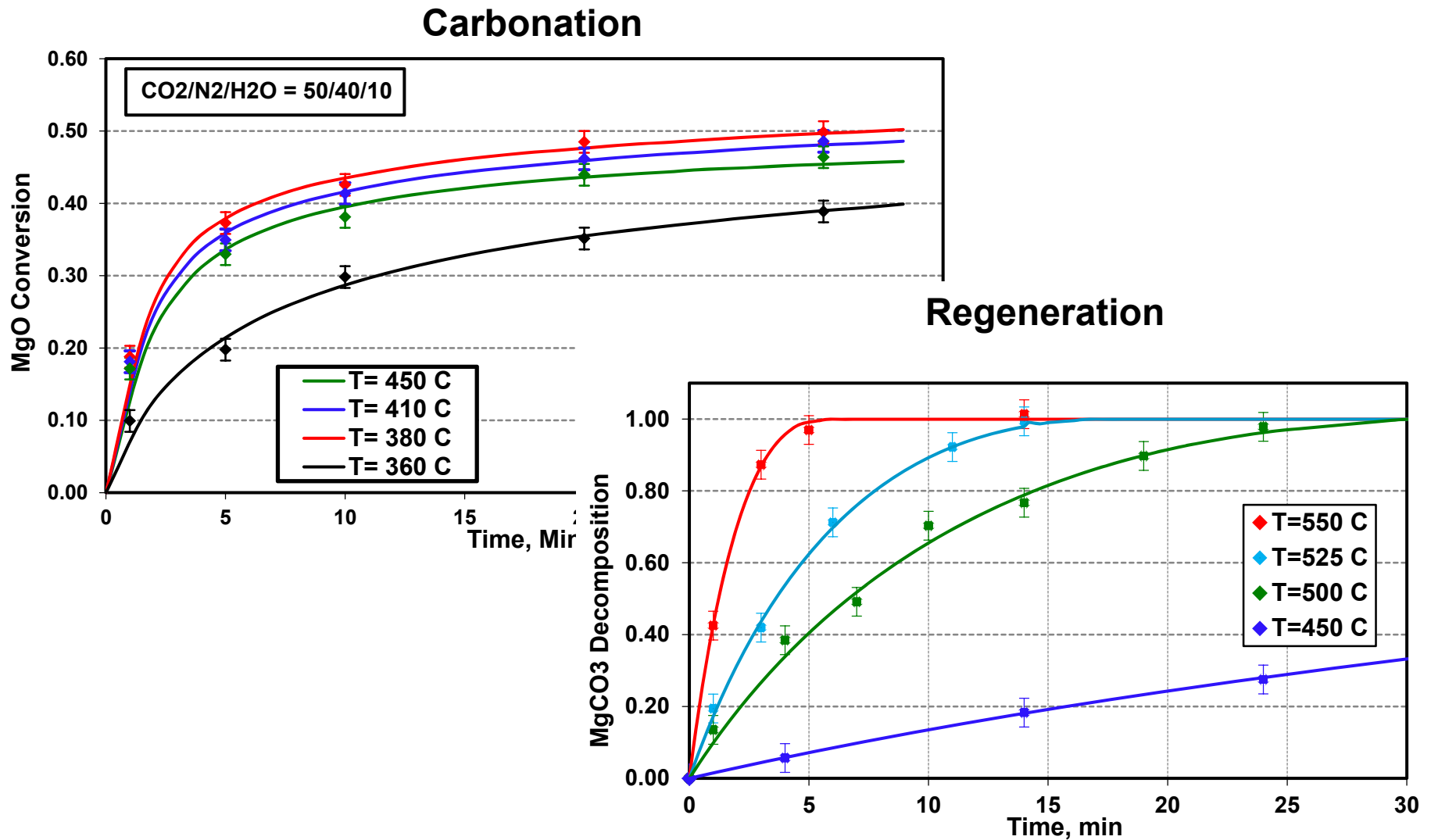
$$\frac{dX}{dt} = -\frac{\frac{3}{r_p} \frac{k_s}{N_{MgO}^o} (C_b - C_e) (1-X)^{\frac{2}{3}}}{1 + \frac{k_s}{D_g} r_p (1-X)^{\frac{1}{3}} (1 - \sqrt[3]{\frac{1-X}{1-X+ZX}})}$$

$$D_g = D_{g0} - \alpha X$$

Abbasi et al., Fuel, 2013

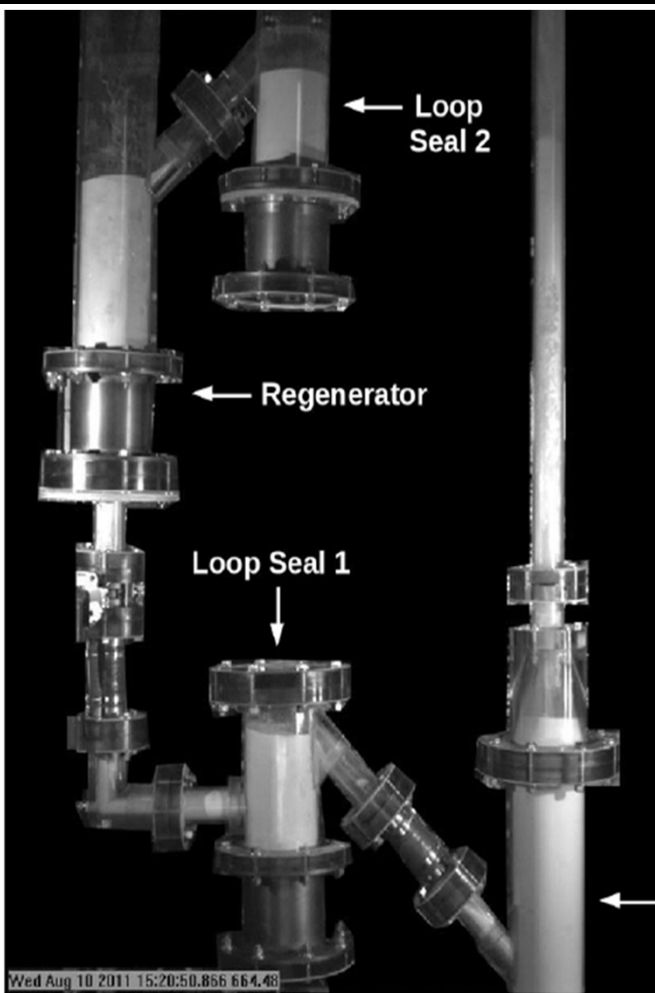
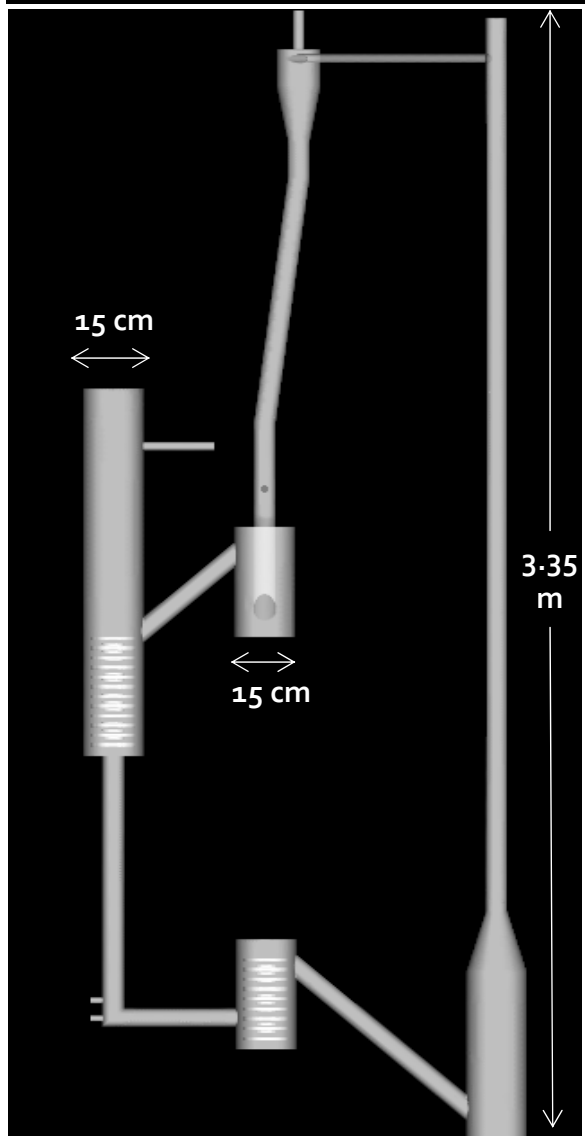
17/29

VDSC Model Fit to Dispersed bed Experiments



Preliminary Base case design and Simulation Results

Full Loop Base Case Design

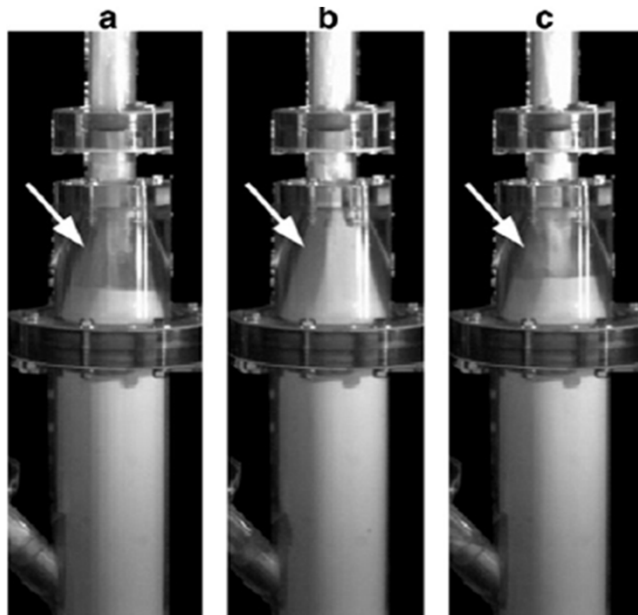


Location	Nominal gas Flow (g/s)
Adsorber	5
Loop seal 1	0.7
Loop seal 2	0.8
Regenerator	1
Move air	0.14

Mean Particle size = 185 μm
Particle density = 2480 kg/m^3

Based on DOE/ NETL Carbon Capture Unit.
(Courtesy of Larry Shadle, NETL)

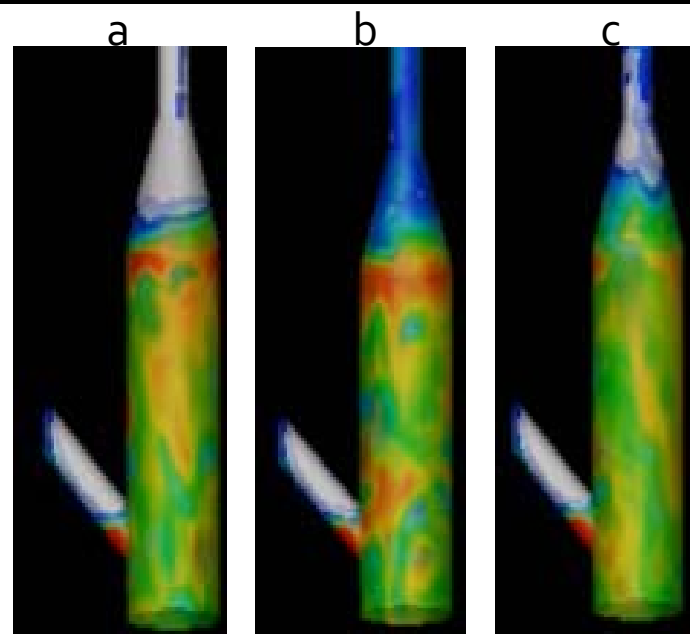
Hydrodynamics of the Absorber



NETL experimental images
every 0.4-0.6 sec

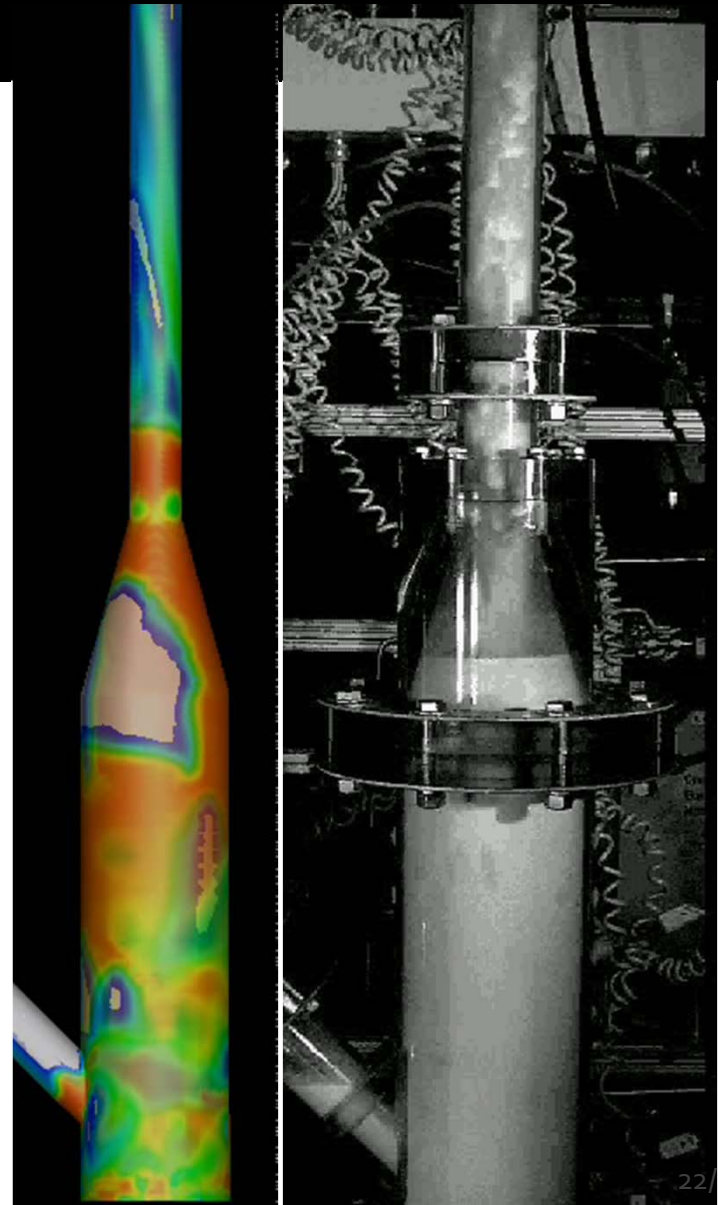
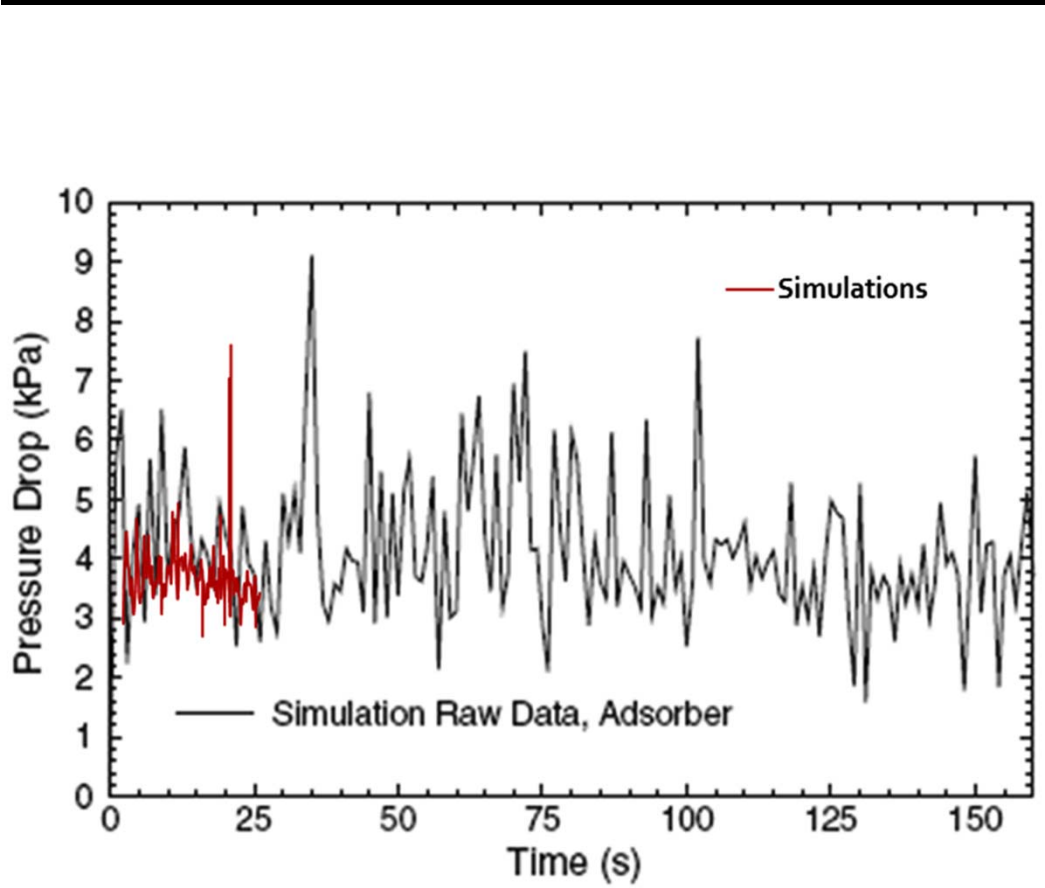
Sequence of events:

- (a) initially empty cone,
- (b) cone plugged with particles
- (c) final empty cone.



“Chugging occurs when a large mass of particles lifts from the fluidized bed and moves into the cone leading into the riser. The cone-constriction prevents particles from flowing smoothly into the riser and particles plug the riser pipe.”

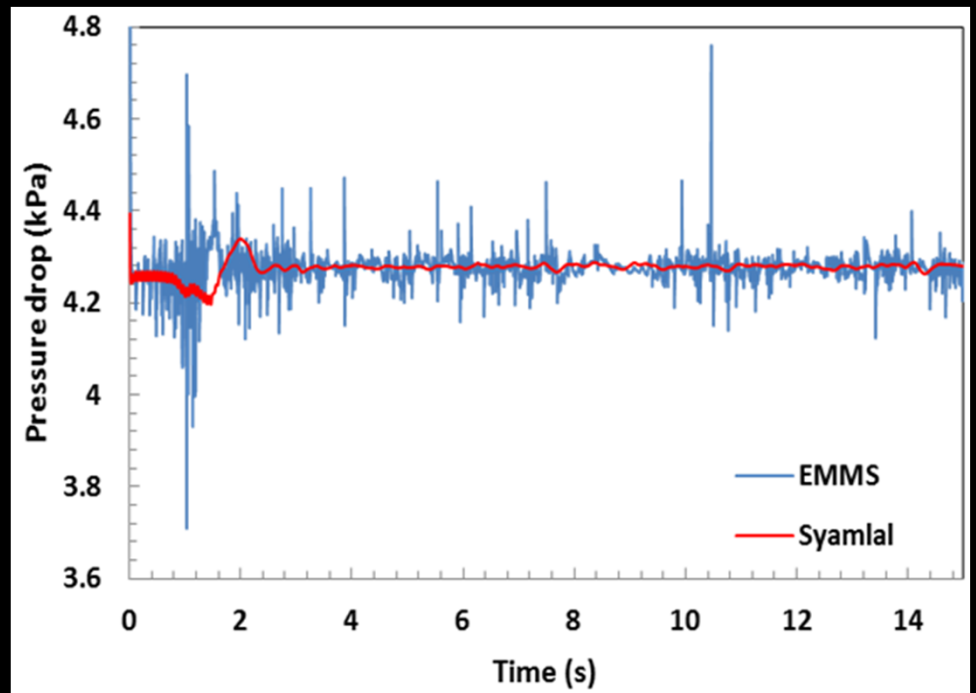
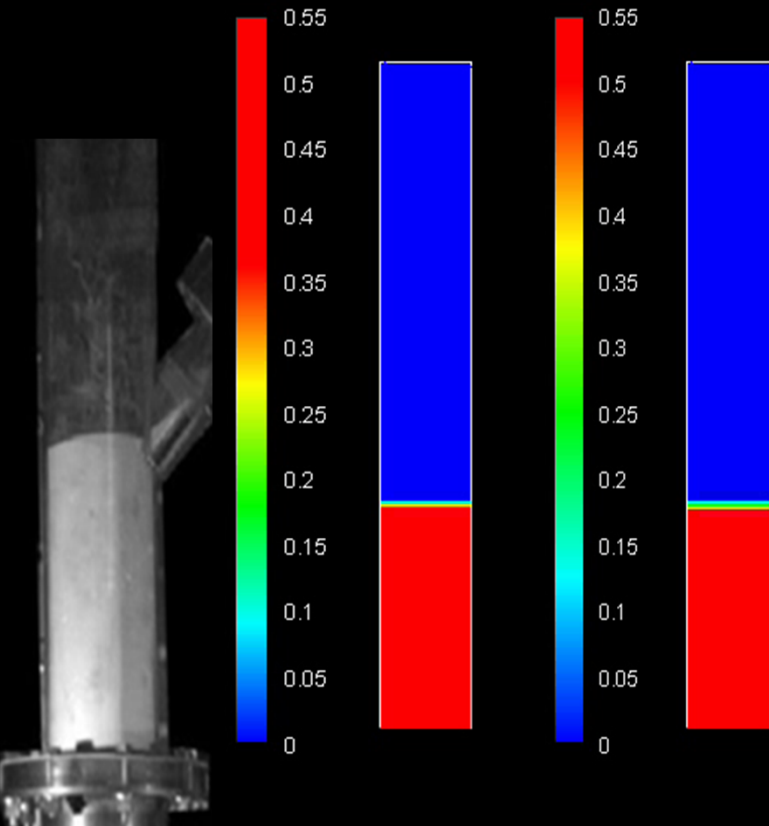
Observed Fluidization Behavior in the Riser



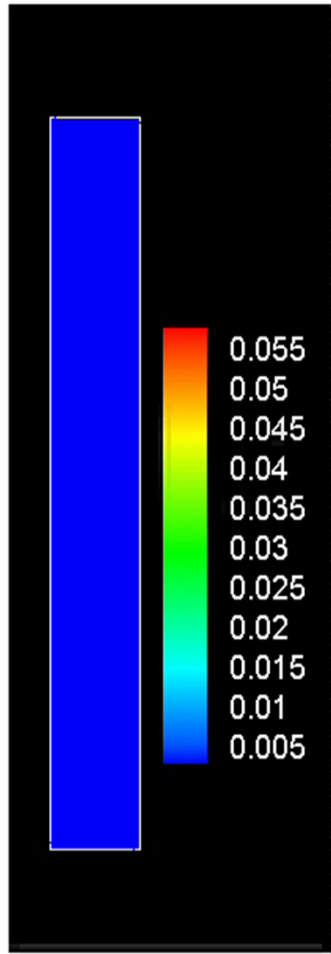
Experimental data reported by Clark et al., *PowderTech*. 2013

Hydrodynamics of the Regenerator

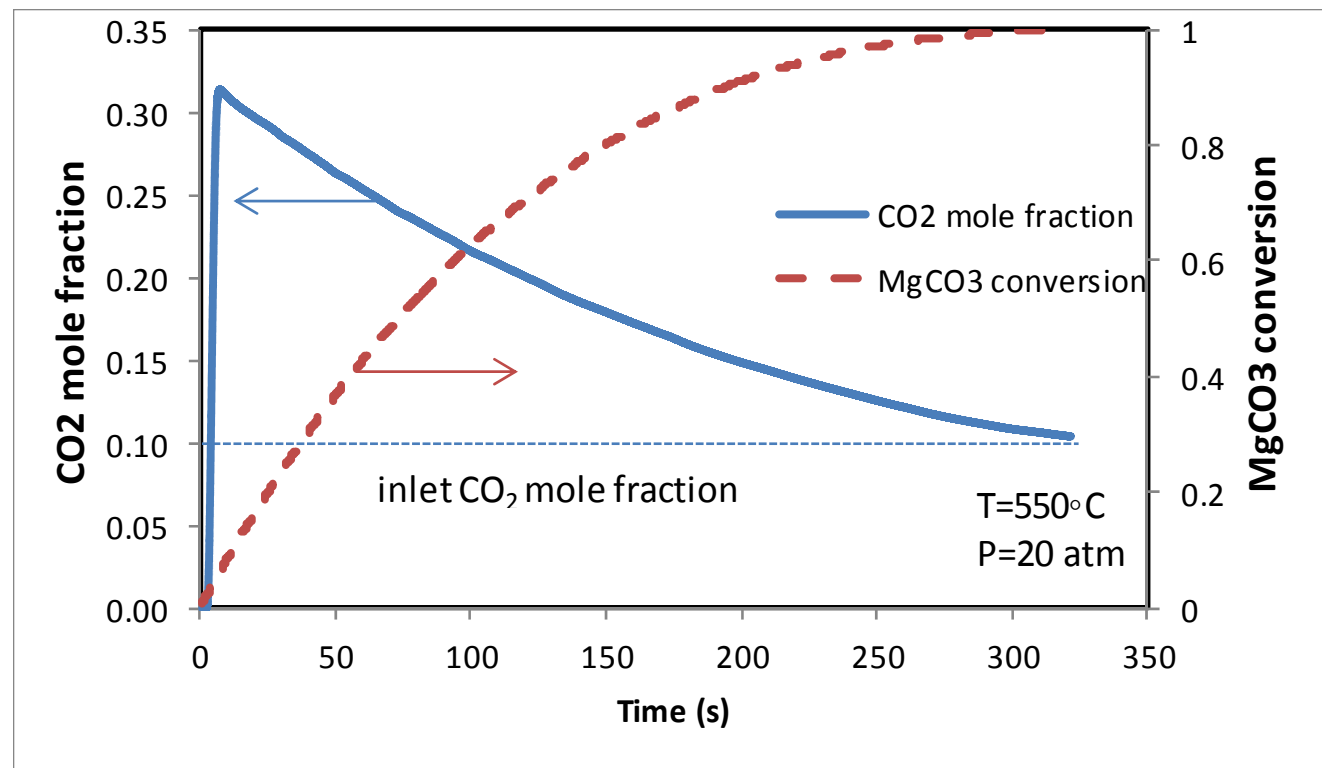
Syamlal-O'Brien EMMS



Batch Regenerator Performance



CO₂ concentration [=] kmol/m³



Effect of Frictional Pressure on L-Valve Hydrodynamics

Schaeffer Model

- bypassing of the fluidizing gas through the lower seal pot

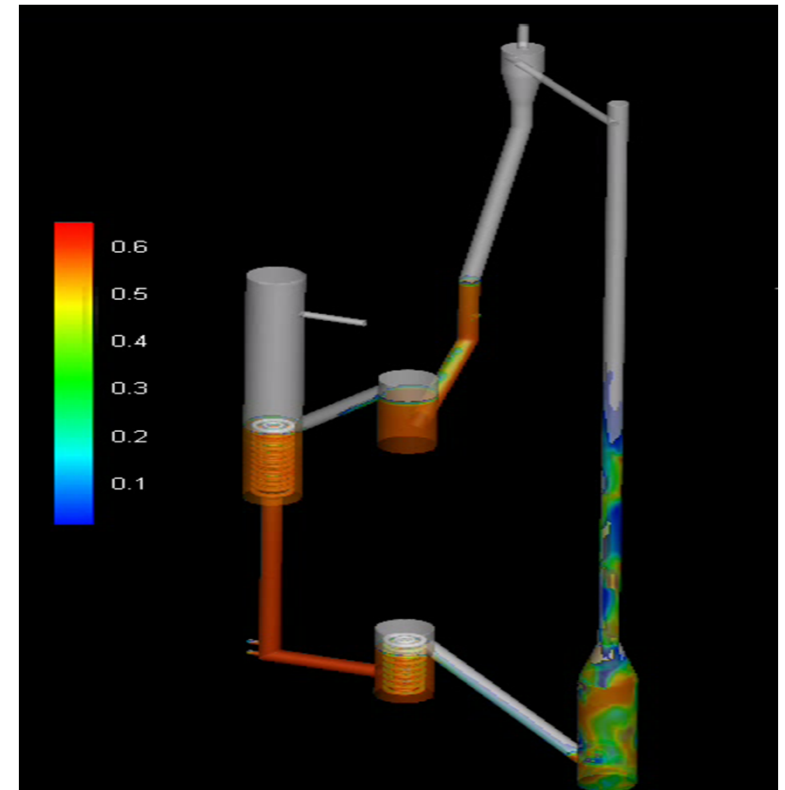
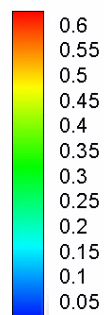
- Bubbling standpipe

$$\varepsilon_s < \varepsilon_{fr} \quad \mu_s = \mu_{kin} + \mu_{col}$$

$$\varepsilon_s \geq \varepsilon_{fr} \quad \mu_s = \mu_{kin} + \mu_{col} + \text{Modified } \mu_{fr}$$

(With Modified Johnson-Jackson frictional Pressure)

Schaeffer Model



Comparison of Frictional Models

Schaeffer frictional model (which is based on coulomb law)
 has two major shortcomings:

- 1) It is discontinuous (solid volume fraction ~ 0.5)
- 2) It is under predicting the frictional viscosity

Schaeffer frictional model

$$\mu = \begin{cases} \varepsilon_s < \varepsilon_s^{\text{fr}} \Rightarrow \mu_{\text{kin}} + \mu_{\text{col}} \\ \varepsilon_s \geq \varepsilon_s^{\text{fr}} \Rightarrow \mu_{\text{kin}} + \mu_{\text{col}} + \mu_{\text{fr}} \end{cases}$$

where

$$\mu_{\text{kin}} = \frac{10\rho_s d_s \sqrt{\Theta_s \pi}}{96\varepsilon_s (1 + e_{ss}) g_0} \cdot \left[1 + \frac{4}{5} g_0 \varepsilon_s (1 + e_{ss}) \right]^2$$

$$\mu_{\text{col}} = \frac{4}{5} \varepsilon_s \rho_s d_s g_0 (1 + e_{ss}) \sqrt{\left(\frac{\Theta_s}{\pi} \right)}$$

$$\mu_{\text{fr}} = \frac{P_s \sin \phi}{2\varepsilon_s \sqrt{I_{\text{DD}}}}$$

Continuous frictional model

$$\mu = \mu_{\text{kin}} + \mu_{\text{col}} + \mu_{\text{fr}}$$

where

$$\mu_{\text{kin}} = \frac{\sqrt{\pi \Theta_s} (d_s \rho_s / 24 \varepsilon_s g_0) (((5 + 2 \varepsilon_s g_0 (1 + e_{ss}) (3e_{ss} - 1)) / ((1 + e_{ss}) (3 - e_{ss})))}{(1 + (45 \mu_g / (6 \varepsilon_s g_0 d_s \rho_s \sqrt{(\Theta_s / \pi)} (1 + e_{ss}) (3e_{ss} - 1))))}$$

$$\mu_{\text{col}} = \frac{4}{5} \varepsilon_s \rho_s g_0 (1 + e_{ss}) \left(\frac{\mu_{\text{kin}}}{\rho_s} + d_s \sqrt{\frac{\Theta_s}{\pi}} \right)$$

Sundaresan frictional model

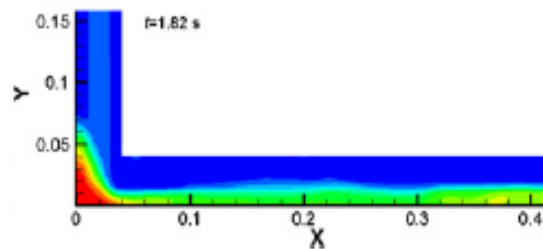
$$\mu_{\text{fr}} = \frac{P_s \sin^2 \varphi}{\varepsilon_s \sqrt{4 \sin^2 \varphi \cdot I_{\text{DD}} + (\nabla \cdot \vec{u}_s)^2}}$$

Laux frictional model

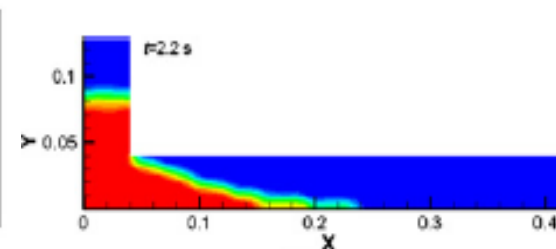
$$\mu_{\text{fr}} = \mu_{\text{Laux}} = \frac{6 \sin \varphi}{9 - \sin^2 \varphi} \frac{3 |\lambda \nabla \cdot \vec{u}_s - \frac{P_s}{\varepsilon_s}|}{2 \sqrt{3 |I_{\text{DD}}|}}$$

Comparison of Frictional Models

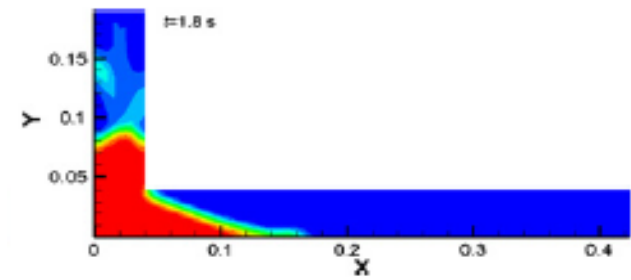
Schaeffer frictional model



Sundaresan frictional model



Laux frictional model



model	Prediction, Angle of Repose
Schaeffer	0
Sundaresan	21
Laux	29.5
Experiment	36

- Investigation of proper modeling of very dense granular flows in the recirculation system of CFBs, Nikolopoulos et al, Particuology, 2012.

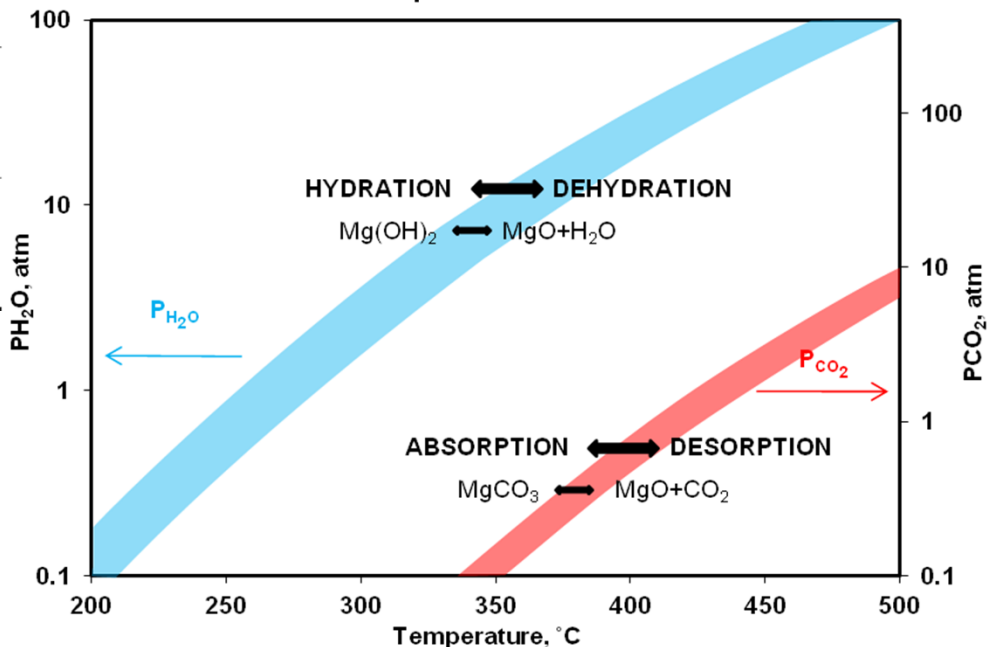
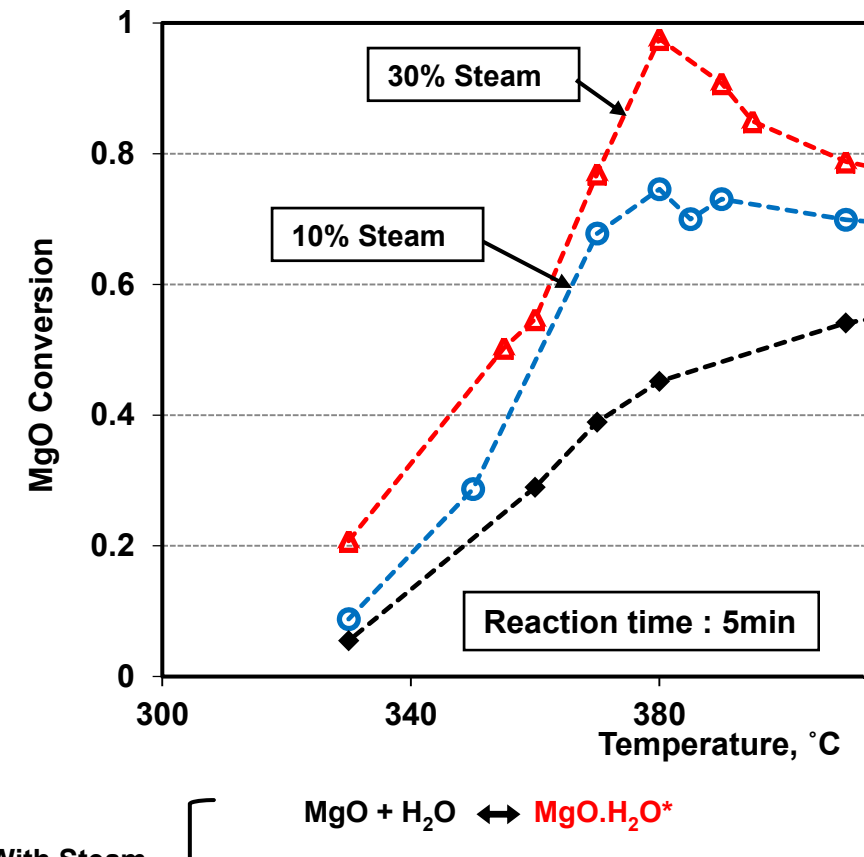
Work to be completed

- Effect of WGS reaction
- Modeling of combined absorption & WGS reactions
- Further modification of solid frictional viscosity.
- Completion of full loop simulation by including reaction and population balance model for density changes.

Thanks for your attention

Questions?

Effect of Steam on Reactivity



Numerical Modeling: Conservation Equations

Eulerian- Eulerian Approach in combination with the kinetic theory of granular flow

Assumptions: Uniform and constant particle size and density

- Conservation of Mass

$$\text{- gas phase: } \frac{\partial}{\partial t}(\varepsilon_g \rho_g) + \nabla \cdot (\varepsilon_g \rho_g v_g) = \dot{m}_g$$

$$\text{- solid phase } \frac{\partial}{\partial t}(\varepsilon_s \rho_s) + \nabla \cdot (\varepsilon_s \rho_s v_s) = \dot{m}_s$$

- Conservation of Momentum

$$\text{- gas phase: } \frac{\partial}{\partial t}(\varepsilon_g \rho_g v_g) + \nabla \cdot (\varepsilon_g \rho_g v_g v_g) = -\varepsilon_g \nabla P + \nabla \cdot \tau_g + \varepsilon_g \rho_g g - \beta_{gs} (v_g - v_s)$$

$$\text{- solid phase } \frac{\partial}{\partial t}(\varepsilon_s \rho_s v_s) + \nabla \cdot (\varepsilon_s \rho_s v_s v_s) = -\varepsilon_s \nabla P - \nabla P_s + \nabla \cdot \tau_s + \varepsilon_s \rho_s g + \beta_{gs} (v_g - v_s)$$

- Conservation of solid phase fluctuating Energy

$$\text{- solid phase } \frac{3}{2} \left[\frac{\partial}{\partial t}(\varepsilon_s \rho_s \theta) + \nabla \cdot (\varepsilon_s \rho_s \theta) v_s \right] = (-\nabla p_s I + \tau_s) : \nabla v_s + \nabla \cdot (\kappa_s \nabla \theta) - \gamma_s$$

Generation of
energy due to solid
stress tensor

Diffusion dissipation

Numerical Modeling: Drag Correlation

Gas-solid inter-phase exchange coefficient: EMMS model (Wang *et al.* 2004)

$$\beta_{sg} = \begin{cases} \frac{3}{4} \frac{(1 - \varepsilon_g) \varepsilon_g}{d_p} \rho_g |u_g - u_s| C_{D0} \omega(\varepsilon_g) & \varepsilon_g > 0.74 \\ 150 \frac{(1 - \varepsilon_g)^2 \mu_g}{\varepsilon_g d_p^2} + 1.75 \frac{(1 - \varepsilon_g) \rho_g |u_g - u_s|}{d_p} & \varepsilon_g < 0.74 \end{cases}$$

Heterogeneity Factor
 $\omega < 1$

$$\omega(\varepsilon_g) = \begin{cases} -0.5760 + \frac{0.0214}{4(\varepsilon_g - 0.7463)^2 + 0.0044} & 0.74 < \varepsilon_g \leq 0.82 \\ -0.0101 + \frac{0.0038}{4(\varepsilon_g - 0.7789)^2 + 0.0040} & 0.82 < \varepsilon_g \leq 0.97 \\ -31.8295 + 32.8295 \varepsilon_g & \varepsilon_g > 0.97 \end{cases}$$

